

CENTER FOR RADIOPHYSICS AND SPACE RESEARCH
CORNELL UNIVERSITY
ITHACA, NEW YORK

September, 1961

FACILITY FORM 802

N66-85332	
(ACCESSION NUMBER)	(THRU)
52	MAPE
(PAGES)	(CODE)
CR 76154	
(NASA CR OR TMX OR AD NUMBER)	(CATEGORY)

PRELIMINARY REPORT ON EXPERIMENTS RELATING TO THE
LUNAR SURFACE

by

Bruce W. Hapke

Sponsored by General Motors Corporation and NASA
Contract Nsg 119-61

PRELIMINARY REPORT ON EXPERIMENTS RELATING TO THE LUNAR SURFACE

I. INTRODUCTION

This report describes the activities and results to date of a series of experiments which were undertaken by the Cornell University Center for Radiophysics and Space Research under the direction of Prof. T. Gold, Director of the Center, and sponsored by grants from the General Motors Corporation and National Aeronautics and Space Administration. The report is divided into two sections. In the first section is presented a brief summary of the contents of recently-published papers which pertain to the nature of the lunar surface. Certain conclusions which may be drawn from this literature survey are also presented, although these conclusions are by no means unique or exclusive. The second section of the report describes the experimental apparatus which has been built or purchased. A summary of the experiments and the preliminary results which have been obtained to date follows.

II. CONCLUSIONS REGARDING THE NATURE OF THE LUNAR SURFACE

The following is a very brief summary of data gathered in a survey of recent papers and some conclusions which can be deduced therefrom. Most of the data was compiled by Hugh VanHorn, a graduate student in the Space Research Center. This section is not intended to be complete. For an advanced general reference concerning the moon see reference 1.

A. Introduction

The general conditions obtaining on the moon are well-known. Our natural satellite is a smaller world than the earth, with a surface gravity about one-sixth that of the earth. Its atmosphere is undetectably small; a recent attempt to measure this quantity gave an upper limit of 6×10^{-13} atmospheres (2). It is not believed to possess a magnetic field, although the absence of such a field

has not been completely verified. Since there is no atmosphere or magnetic field to protect it, the surface of the moon has most certainly been influenced by micrometeorite bombardment and by solar radiation in the form of electromagnetic radiation - in wavelengths from infrared through soft x-rays - and hydrogen plasma in the form of protons of energy around 10 kev. The proton density in the plasma is probably $10\text{-}100\text{ cm}^{-3}$ during periods of low solar activity and rises to greater than 1000 cm^{-3} following flares (3). The major features of the moon, e.g., the craters and maria, are believed to have been caused by great collisions of meteorites and planetesimals with the moon (4), although many authorities still hold that these features were shaped by some form of vulcanism.

B. Radar Measurements

Radar echoes have been detected from the moon on many wavelengths from about 10 cm. to 3 m. (5-13). The surprising result from these measurements is that the radar pulses appear to be reflected specularly. That is, on a scale of several centimeters the moon appears to be very smooth with a rms slope of less than 5° . The echoes are returned primarily from a small area around the sub-earth point, the somewhat mountainous region to the south of Mare Vaporum. This rms slope is certainly much smaller than that of terrestrial terrain, especially mountainous terrain. It implies that some agency is continuously at work filling cracks and craters and leveling the surface.

The second surprising features of the radar experiments is the low reflection coefficient of the lunar surface. By analyzing the leading edges of the echoes of various wavelengths Senior and Siegel (5) have deduced that the mean dielectric constant is about $k = \epsilon/\epsilon_0 = 1.08$ and that the conductivity is $\sigma = 4.3 \times 10^{-4}$ mho/m. Not too much importance should be attached to the value for the latter quantity, since the data could be fitted almost equally well by a surface of zero conductivity.

The low value for k implies that the surface consists of a layer of material of considerable depth in a very low state of compaction. Brunshwig et al (14) have measured the dielectric constants of a number of rocks in various forms. From their data one can infer that in order to obtain such a low dielectric constant the average density of the minerals in the layer must be of the order of $1/20$ of that of solid rock.

The depth of this loose layer is unknown. If Senior and Siegel's value for σ is taken seriously one obtains a skin depth for radar wavelengths of the order of $\delta = (2/\mu\omega\sigma)^{1/2} \sim 15$ m. Even without using this conductivity one can infer that the layer is probably at least several wavelengths (e.g., several meters) thick, for if the layer were substantially thinner the radar pulses would be returned from the solid underlying rock.

It is also of interest to note that this conductivity is a couple orders of magnitude higher than that of most plutonic rock (15). However, if the layer consisted of material which had been subjected to a considerable dose of ionizing radiation the electrical conductivity would be considerably increased over its natural value.

C. Thermal Emission Data

Thermal blackbody radiation from the moon has been measured in the near infrared ($8-14\mu$) (16-19), and at radio wavelengths between about 1.5 mm and 75 cm (20-33).

In the infrared the surface heats up and cools off extremely rapidly with any change in the incident solar radiation, as during an eclipse. This implies that the upper layers of the surface are poor conductors of heat. From an analysis of Petit and Nicholson's data Wesselink (34) has concluded that the material comprising the topmost layers has $K\rho C \sim 10^{-6} \text{ cal}^2 \text{-cm}^{-4} \text{-sec}^{-1} \text{-deg}^{-2}$, where K = thermal conductivity, ρ = density, and C = heat capacity per gram.

The only materials with such low thermal constants are dust in vacuum and possibly also foams.

The emissivity of the surface is close to unity; since the emissivity of most rocks is around $1/2$ (1), this implies that on a scale of infrared wavelengths (10μ) the surface is extremely rough with many cavities.

There appears to be little difference in the thermal behavior of maria and highlands, indicating that both types of surfaces are covered with a similar insulating layer. The exception to this statement is Tycho and a few other new-looking craters. These areas do not heat up and cool off as rapidly as their surroundings, implying that the insulating layer is thinner there. Sinton concludes that his observations are consistent with a layer of dust 0.3 mm thick over solid rock in areas in Tycho but that the layer is much thicker elsewhere.

While infrared radiation can monitor only the uppermost layers, radio wavelengths can "see" below the surface. The equivalent black body temperature of the moon as deduced from the radio-thermal measurements consists of a constant component and a time-varying component. The constant component of temperature measured by most of the observers is between 200°K and 250°K . The amplitude of the varying component decreases with increasing wavelength and its phase lags the lunar phase by an angle which increases with wavelength.

There have been a few attempts to calculate the vertical temperature profile under the lunar surface using the thermal-emission data (26, 35). Usually a model for the profile of the form

$$T(x,t) = T_c + T_v e^{-\beta x} \cos\left(\frac{2\pi}{T} t + \alpha x\right)$$

is assumed, where x is the depth under the surface, t is the time ($t = 0$ at full moon), T = one month, and T_c , T_v , β and α are parameters which are determined by matching the model to the data. The thermal scale height $1/\beta$ found in this manner

is of the order of 10-30 cm. However, not too much importance should be attached to this model since it assumes that the thermal and electrical constants of the lunar surface K , ρ , C , k and σ are independent of depth and temperature. This assumption will not hold if the composition or density changes with depth or if appreciable heat is conducted by radiation, in which case K is proportional to the cube of the temperature. Jaeger and Harper (33) have emphasized the need for a model consisting of solid rock overlain with a thin layer of dust.

D. Reflected Sunlight

Sunlight in the near ultra-violet and visible reflected from the surface of the moon has been measured in many ways, and numerous attempts have been made to match the lunar reflection characteristics with terrestrial materials. The lack of success in this last endeavour has been conspicuous.

Stair and Johnston (36) found two absorption bands in the ultra-violet spectrum and felt that this indicated the presence of powdered glassy silicates and traces of iron on the lunar surface. Wood (37) found many areas on the moon where the relative brightness was different in visible and UV. He thought that sulfur-bearing minerals might be present.

In the visible, the moon has an extremely low albedo of the order of 7% for the maria and 14% for the highlands. Except for albedo there is little difference in appearance between the maria and the highlands (38). Indeed, the moon seems to affect the spectrum of the sunlight very little.

The unique light-reflecting properties of the moon may furnish an important clue to the nature of the lunar surface. The intensity of reflected sunlight as a function of the angles to the normal to the surface of observation and illumination have been measured by Bennet (39) and Van Diggelen (40). There appears to be little difference in the reflecting properties of various portions of the surface of the moon. These investigators attempted without success to duplicate the measured reflection laws using a wide variety of terrestrial materials, as did

Sytinskaya (41) and Barabashov and Chekirda (42). The latter authors studied rocks in their natural state, after irradiation with photons and protons, after melting in air and in vacuum, and after pulverizing into grains of various sizes. The material must closely matching the lunar surface was found by Van Diggelen to be a species of lichen. The lichen has a structure which is rough, scraggly and branching. A surface consisting of a flat plate in which many tiny pits had been drilled, and which one would expect might duplicate the appearance of rock bombarded by micrometeorites, gave a poor fit to the lunar data.

The fact that the full moon is of equal brightness all across its face indicates that the lunar surface is very rough on a scale of the wavelength of visible light (0.5μ). This is in contrast with the radar data which implies that the moon is smooth on a scale of tens of centimeters. Thus it can be inferred that the surface material has a microstructure with a scale somewhere between 1μ and 1 cm.

The amount by which the moon polarizes the sunlight reflected from it has been measured by Lyot (43), Dollfus (44, 45) and Wright (46). All areas on the moon exhibit a similar behavior. The percent polarization is always low and the polarization curve with lunar phase is symmetric about full moon. The percent polarization is zero at full moon, becomes negative on either side of full moon, reaching a minimum of a few percent at about $\pm 10^\circ$, then becomes positive going through a maximum of around 10-18% (depending on the area) at about $\pm 100^\circ$.

As with the reflection laws, this behavior could not be duplicated by terrestrial materials nor by meteorites. In all cases the surfaces polarized the light too much. Wright found that when crushed rocks were observed, the polarization decreased with decreasing particle size and with increasing surface roughness.

E. Discussion

From the preceding summary of measurements relating to the lunar surface it appears that the outer portions of the moon consist of a surface layer of extremely low density underlain by a denser material which may be either bedrock or solidly compressed powder. Two problems are of immediate interest, the chemical composition and distribution of the underlying material, and the origin, nature, depth and distribution of the loose layer.

At one time it was thought that there was bedrock of two types. The maria were supposed to be lava flows of darker-colored basic rock while the highlands were lighter-colored acidic rock. Although this supposition is certainly possible, it is not necessarily true. Both the maria and the highlands appear to be covered with some sort of soil and any difference in appearance may well be due to differences in the soil rather than in the underlying rock. Besides, there are doubts about the existence of lava flows on the moon. There are many indications that the moon may never have had a molten interior (1). It has been proposed that the lava was created by the heat generated by the great meteor collisions which gave birth to certain maria. This possibility also appears doubtful. Studies of terrestrial meteor craters (47) show no signs of extensive melting nor of causing a break in the earth's crust through which lava could flow, even though in the case of the Vredefort crater in South Africa there was enough kinetic energy available to do so.

Clues as to the composition of the bedrock come from three sources. (1) Both the earth and the moon may have been accreted from the same substances, in which case one would expect the moon to be of similar composition to the interior of the earth; e.g. a basic rock similar in composition to chondritic meteorites. (2) The chondritic meteorites may be debris left over after the formation of the planets. They are an ultrabasic rock similar to peridotite with some metallic iron and nickel (1). (3) The stones known as tektites may be material knocked loose

from the moon by meteor collisions (48). These stones have a high silica and alumina content and very little water.

The lunar soil overlying the denser material cannot be solid rock because the density and thermal constants are too low. The most likely hypothesis is that the surface layer is dust eroded from the bedrock by some agency. It has also been proposed that the layer consists of hardened foam, "meteoric slag", and of whiskers. We will discuss each of these proposals briefly.

(1) Foam: Firsoff (49) has suggested that large areas of the moon are covered with foam generated when lava carrying large amounts of adsorbed gases reached the surface. This hypothesis is doubtful, however; for while it might be possible that some areas (such as the maria, if they are lava flows) are covered with foam, it is difficult to see how the foam could be generated over the whole lunar surface. Yet it would be necessary to have almost the entire moon covered including the mountainous slopes of the highland areas.

(2) Meteoric slag: Sytinskaya (41) has proposed that the lunar surface is a rough, jagged layer of fused and partially vaporized rock resulting from the continuous bombardment of micrometeorites. This author assumes that the vaporized rock from the micrometeorite collisions reacts chemically with the surface of the bedrock to change the composition and appearance of the upper layers vastly. This hypothesis is possible, particularly since it is not known what the effect of prolonged bombardment of high-velocity particles on a surface will be. However, terrestrial experiments on hypervelocity impact (50) indicate that the craterlets thus produced are not dissimilar to the visible craters on the moon. Such a surface would not be jagged enough to produce the light-reflecting properties of the moon. It is also difficult to see how a layer sufficiently thick to cause the low dielectric constant could result from this mechanism alone, nor does this proposal seem able to explain the smoothness of the surface on a scale of tens of centimeters.

(3) Whiskers: It has been suggested that the man in the moon might have whiskers of mineral crystals (51). It is well-known that when a crystalline substance is sublimed from a tenuous atmosphere of its own vapor the crystals tend to form long thin needles or whiskers. This atmosphere of rock vapor might result from the sputtering of molecules from the lunar surface by the solar protons, or it could also be produced in the collisions of micrometeorites with the lunar surface.

A second mechanism for growing whiskers might also be due to the irradiation by the solar plasma. Under ionic bombardment it has been found (52) that surface atoms of the target material tend to migrate extensively and conglomerate around surface defects. In some cases whiskers have been observed to start from these defects. The whiskers are around 15μ in diameter.

A whiskery surface would be extremely rough on the scale of 1μ but would appear quite smooth on the scale of several centimeters. Whiskers could grow out sideways from hills and crater walls to fill in depressions, and the resulting structure would be of low average density. It is difficult to see how this sort of structure could grow whisker upon whisker to a depth of several meters, as required by the radio evidence except by the continual influx of fresh meteoric material. This however would produce a completely uniform composition and structure for all areas of the lunar surface. This leaves then no way of accounting for the different albedo of the maria and the mountainous highlands, since neither composition nor surface treatment would have been different.

(4) Dust: A dusty surface could be created by material eroded from the bedrock by various agencies, of which meteoric impact is probably the most important. The size of the dust particles composing the layer is unknown, although from an analysis of Petit and Nicholson's data Wesselink (34) has estimated that an upper limit to the particle size is 200μ . The terrestrial experiments on

hypervelocity impact (50) indicate that a good deal of small solid debris is ejected from the surface by the collision. For micrometeorites of the order of 10μ or less in size (53) most of the debris would be of the order of 1μ or less in diameter. The dust would probably clump together due to electrostatic effects to form objects which are large compared with 1μ and which could give a rough surface on a scale of visible and infrared wavelengths.

Rock powders in vacuum seem to have the right thermal values (54). If the surface layer consists of rock powder then we may estimate the thermal constants of the dust as follows. Wesselink's analysis indicates that the product $K\rho C$ is of the order of 1×10^{-6} cgs units, whereas the work of Brunschwig et al (14) implies that the rock is in an uncompacted form with density approximately $1/20$ that of solid rock. Most rocks have $C \sim 0.2$ cal/gm/deg (55) and $\rho \sim 3$ gm/cc (14). Reducing the density by 20 gives $\rho C \sim .03$ cal/cc/deg. Hence $K \sim 3 \times 10^{-5}$ cal/cm/deg. If the model for the vertical temperature profile described previously is valid, these values for the thermal constants give a vertical thermal scale height $1/\beta$ of $1/\beta = (\pi \rho C / TK)^{1/2} \sim 30$ cm.

The light-reflecting properties of pulverized rock have been investigated by various persons but the agreement with those of the moon was poor. However dust deposited under high-vacuum conditions has not been studied at all. One expects a priori that the appearance of such a surface will be considerably different from air-deposited dust. Tiny particles in air have surface layers of adsorbed air and oxides which can act as a lubricant and allow the dust grains to slide over one another and thus to compact more tightly. But in a hard vacuum with no adsorbed surface layers between them, two particles may tend to weld wherever they touch. Hence vacuum-deposited dust may form very loose, open structures of low density. Also, because of this high possible cohesion and adhesion the dust may be able to cling to very steep slopes, such as the sides of the famous Straight Wall.

From satellite measurements (53) it may be estimated that the flux of 10μ diameter micrometeorites in space at 1 AU from the sun is of the order of 10^{-6} $\text{cm}^{-2}/\text{sec}$. Hence in 10^9 years enough material has impacted on the lunar surface to deposit a layer several meters thick. Each impacting particle will probably create several times its own volume in dust.

The actual existence of such a thick layer depends on whether or not the dust can be transported away from large areas in order to expose fresh rock to the micrometeorites. If no transport mechanisms exist then the bedrock would soon be covered with a shielding layer of debris and the only effect of succeeding impacts would be to stir up the dust a little. Only a few centimeters of dust would be sufficient to shield the rock from further erosion. However, if the dust can be transported away from high areas as fast as it is formed then the highlands would be constantly undergoing slow erosion and the low areas filling up with eroded material, possibly to depths of several kilometers.

Another erosion mechanism for producing fine dust may be due to the solar proton bombardment. There are at least three plausible ways in which this irradiation could create dust from solid rocks. (1) The formation of whiskers has already been discussed. These whiskers would be rather fragile and could easily be broken off by flying debris from the micrometeoritic collisions. (2) Natural rocks are often polycrystalline mixtures of minerals of varying hardness. The plasma might preferentially erode one mineral by sputtering or chemical change, thus freeing the more resistant variety in the form of small crystals. (3) The protons have only a short range in rocks - less than 1μ . Thus all protons are brought to rest a short distance below the surface. In stopping they create dislocations and themselves become foreign interstitial atoms in the crystalline lattice when they pick up an electron. After a short time an appreciable impurity concentration of hydrogen would be built up under the surface. For

instance, in less than a year the concentration of atomic hydrogen in the upper micron of the surface would be of the order of one percent by number. These radiation damage effects could change the mechanical properties, such as the lattice spacing or thermal expansion coefficients, sufficiently to cause the irradiated portion of the crystal to pull away from the underlying parts and eventually to flake off in chips of thickness less than a micron.

The lunar surface is certainly being eroded by sputtering induced by the protons. In 10^9 years a layer several meters thick may have been sputtered away. Since the sputtered atoms are emitted with energies of the order of electron volts they have velocities of the same order as the velocity of escape from the lunar surface; hence much of the sputtered material has been lost from the moon.

The thickness of the dust layer and evenness of the surface inferred from the radar measurements implies the existence of one or more erosion and transport mechanisms which erode the dust from high surfaces and carry it to depressions. At least three mechanisms have been proposed.

(1) It has been suggested (1) that the dust particles may be caused to dance downhill by vibrations associated with the micrometeorite impacts. There seems to be no data available on whether appreciable quantities of dust could be transported in this manner.

(2) Gold (56) has suggested transport by electrostatic effects. Because of secondary electron emission from the dust due to ultra-violet and proton irradiation adjacent dust particles could acquire high enough electric charges to levitate against the moon's gravity and glissade down slopes. This mechanism has been investigated somewhat by Grannis (57), who concludes that it could provide fairly large transport rates. However, this rate depends on certain parameters, such as the secondary electron emission coefficients of minerals, which are not known at the present time.

(3) Several persons have suggested that the extreme thermal variations on the moon will be sufficient both to break up rocks into fine dust and transport the dust downhill by thermal expansion and contraction. The thermal forces involved are too small to cause break-up of the rock beyond a size of centimeters, and dust transport by this means appears to be far too slow to account for the probable amount of erosion.

All of these postulated transport mechanisms assume that the dust particles are lying fairly loosely on the surface. The transport rates will be reduced greatly if the particles have a high cohesion and are welded relatively tightly together. Indeed Whipple thinks that the effect of the plasma and micro-meteorite bombardment will cause chemical changes in the outer layers of the dust which will result in a rather strong crust. Apparently this is Sytinskaya's view also. Platt (58) points out that such a surface may be chemically unstable and highly reactive. However there is no experimental data on this matter.

F. Conclusions

In summary, while other possibilities cannot be excluded, the observations indicate that the lunar surface consists of a layer of dust which has been eroded away from the denser underlying material. This material is probably a type of rock similar in composition to chondritic meteorites. The radar data implies that the dust layer is quite thick, at least in places. This implies the existence of a transport mechanism which moves the dust from the higher areas to the lowlands, leaving a layer only a few centimeters or millimeters thick on the highlands but many meters in depth in the maria and in the bottoms of older craters. This hypothesis is supported by the recent radio-thermal investigations of Coates (59) who found that the maria undergo more rapid temperature variations than the mountainous regions. This implies a lower thermal conductivity and thus greater depth of the dust layer in the maria than in the highlands. From the radar and visual data it may also be inferred that this surface layer

may be built up from tiny dust grains welded together at a few points and in an extremely loose state of compaction. Hence the surface in the lower areas may not be capable of supporting large bearing pressures.

III. EXPERIMENTS RELATING TO THE LUNAR SURFACE

A. Introduction

A number of questions presented themselves during the preceding discussion, many of which can be answered by experiments in terrestrial laboratories. The Cornell University Center for Radiophysics and Space Research has undertaken a series of experiments intended to find answers to some of these questions.

1. Properties of vacuum-deposited dust, such as its density, compressibility, cohesion and internal friction.
2. Erosion of lunar-type rocks by solar radiation. Studies of rates of formation of dust and sputtering by protons of energies around 10 kev.
3. Transport of dust by electrostatic effects. Study of the effects of 10 kev protons and ultra-violet radiation on surfaces of small particles of dust. Measurement of the secondary electron emission coefficients from minerals when bombarded by protons, electrons and electromagnetic radiation.
4. Photometric Studies. Measurements of the intensity and polarization of visible light reflected from various surfaces as a function of the angles of incidence and observation, and attempts to duplicate the reflecting properties of the lunar surface.

B. Apparatus

1. Ultra-high vacuum system. The experiments on the rock dust require the elimination of the effects of the particles' previous history in the terrestrial atmosphere. Since the surface films of adsorbed gases change the adhesive properties of the dust grains, it is necessary to reduce them as much as possible in order to simulate lunar conditions. It has been found that bake-out of the experimental apparatus and operation of the vacuum system at 10^{-8} mm Hg or less are required to eliminate these effects.

A high vacuum system* was set up to permit experimentation at the low pressures required. The vacuum chamber is a stainless steel bell jar 18" in diameter and 24" high. Two observation ports are located near the top of the chamber. The jar can be enclosed by a furnace and the jar and its contents baked out at a controlled temperature. The system is actually two vacuum chambers: the ultra-high vacuum volume in the bell jar and an intermediate vacuum buffer system located below the jar. All feed throughs, including electrical, mechanical and water, are first brought through the intermediate vacuum region to minimize the effects of any possible leaks. There are provisions for 20 electrical feed-throughs, 5 rotary-motion feed-throughs and one two-tube cooling water feed-through. At the top of the bell jar is a flange which can be removed and the proton gun installed. The main pump is a 1500 l/sec diffusion pump. The chamber is also lined with coils which can be filled with liquid nitrogen for cryogenic pumping. The system is guaranteed to be able to attain pressures below 1×10^{-8} mm Hg and has been reported to operate in the 10^{-10} mm range. The ultra-high vacuum system is shown in Figure 1.

2. Remote Hook. Three of the rotary-motion feed throughs into the UHV are used to drive an arm with three degrees of freedom and terminating in a hook. This hook can be used to manipulate various objects placed inside the UHV chamber. Thus a number of different experiments can be performed during the same high-vacuum run.

*

The ultra-high vacuum system which was generously purchased by the General Motors Corporation for the Center's use was built by the NRC Corporation of Newton, Massachusetts.



Fig. 1. High Vacuum Chamber and Associated Equipment

3. Telemicroscope. The visual inspection of minute details of objects and surfaces inside the vacuum chamber is important. Hence a long range microscope has been constructed. The principle of this microscope is as follows (see Figure 2). A high quality achromatic collimating lens C is placed a

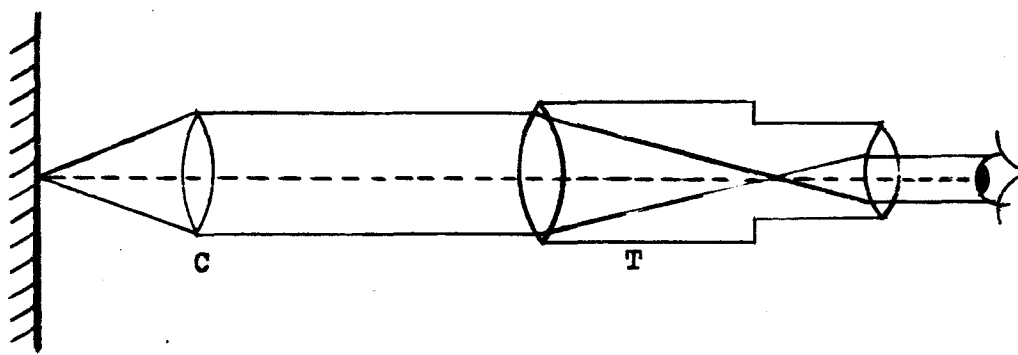


Figure 2. Schematic diagram of long-range microscope.

distance equal to its focal length from the surface being examined, so that the rays from objects on the surface are focussed at infinity. These light rays can then be looked at from any convenient distance with an ordinary telescope T focussed at infinity. With this arrangement, if the magnifying power of the telescope is M then an observer at the eyepiece of T sees an image of the surface which is M times as large as it would appear if his eye were located at the position of C.

In our apparatus the telescope is a Bausch and Lomb Balscope with a turret eyepiece allowing the magnification M to be conveniently varied between 10 X and

and 100 X. The telescope is mounted on a box which fits over one of the port-holes in the bell jar. Between the telescope and the port is a first-surface mirror which reflects light coming out of the port into the telescope. The mirror can be tilted and rotated so that large portions of the chamber can be scanned without moving the telescope.

The telemicroscope has two collimating lenses. One is a 24-1/2" focal length lens for low-power, large scale viewing which can resolve objects down to about 10 μ apart. This lens is located outside the UHV in the same box as the mirror and telescope. For higher power viewing this lens can be removed and a collimating lens with shorter focal length equal to 26 mm used. This second lens is located inside the vacuum chamber and can be moved by the remote hook to a position immediately above the surface of interest. In this way objects of size less than one micron can be examined. The external part of the telemicroscope is shown in Figure 3.

4. Proton Gun. The proton gun is a modified Penning discharge capable of producing a beam of ionized hydrogen of several hundred microamperes. A schematic diagram of the gun is shown in Figure 4. In its conventional form the Penning discharge consists of a cylindrical anode placed between two cathodes and held at a high positive voltage with respect to them. A magnetic field is applied parallel to the axis of the system.

Electrons are emitted from the cathodes by cold-cathode discharge and are attracted into the region of the anode. If they make no collisions there they continue on toward the opposite cathode. However, they now find themselves in an electrostatic field which opposes their motion, and they are repelled back toward the anode, being always constrained by the magnetic field to travel in a tight helix parallel to the axis. This cycle is repeated several times. Thus the path length of the electrons is quite long and the probability of their

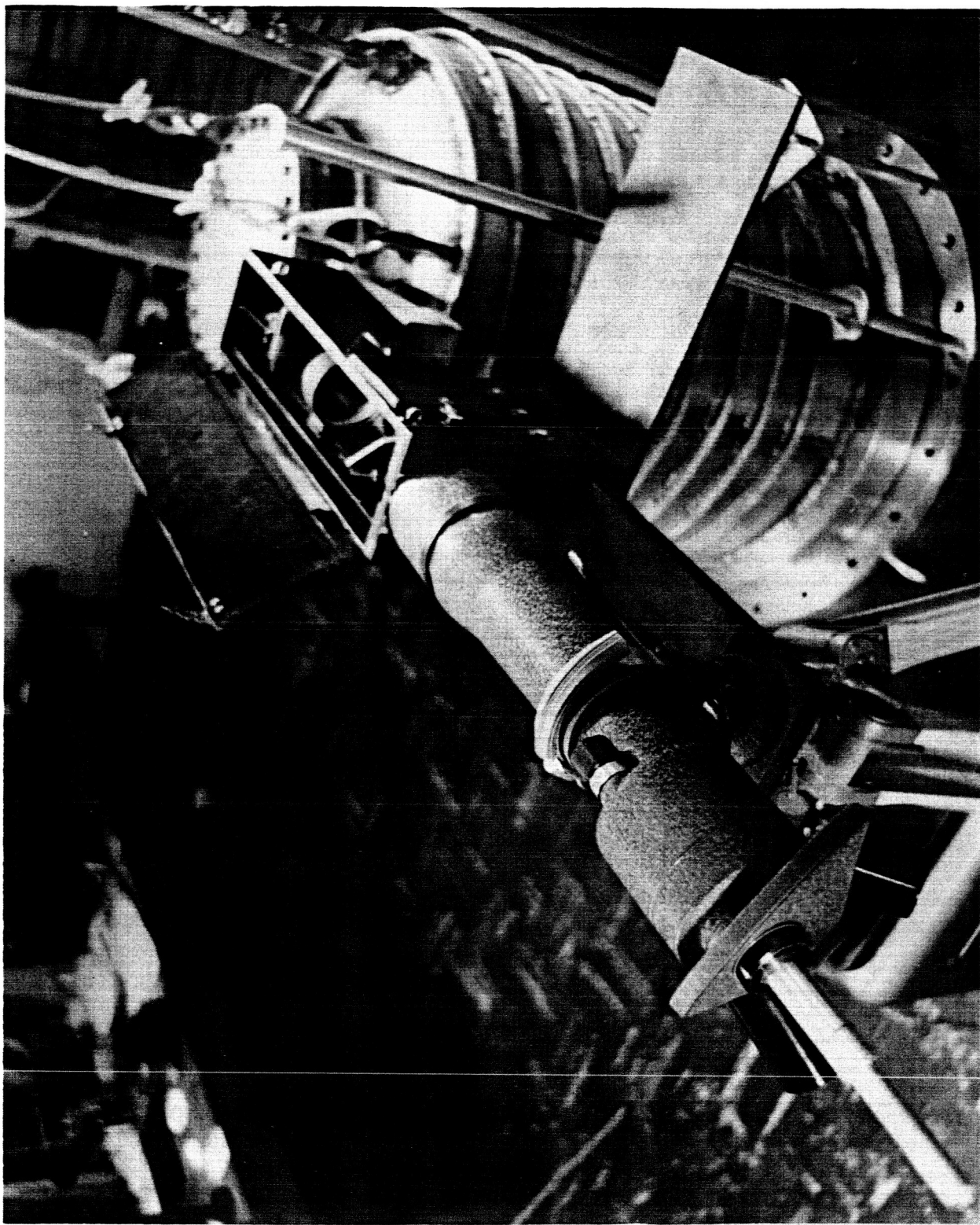


Fig. 3. Telemicroscope Assembly

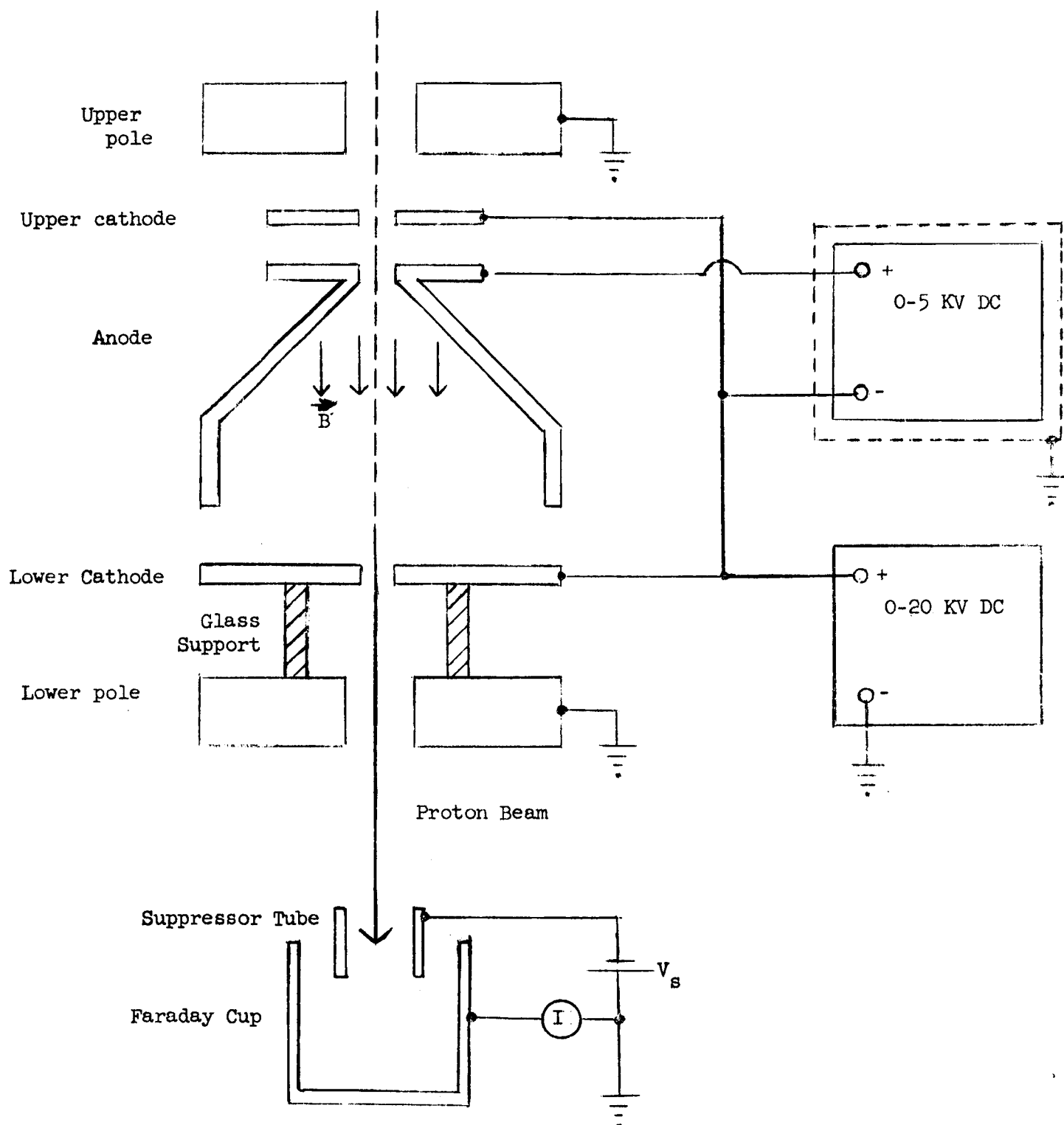


Figure 4. Schematic diagram of proton gun.

undergoing an ionizing collision with a neutral atom of gas in the tube is high. Positive ions created by such collisions, finding themselves on a potential hill, are rapidly accelerated toward one of the cathodes and can be extracted through a hole in the cathode.

During the design of the gun it was realized that creating a small downward axial electrostatic field in the region of the anode should increase the current which could be drawn from the gun in two ways. First, more ions would be started downward than upwards and could be extracted from the gun if such a field existed. Secondly, there are indications that electrons tend to congregate in the region of the anode and to depress the voltage there by space-charge effects, perhaps to the extent of making a shallow potential well for ions (59). Such a well would decrease the extracted ion current, but might possibly be reduced or eliminated by an axial anode field. This field could be created most easily by making the anode a cone instead of a cylinder.

The whole discharge can be raised to up to 20 kv above ground. After emerging from the hole in the lower cathode the hydrogen ions are further accelerated by the lower pole, which is held at ground potential, and are extracted through a hole in the lower pole.

All electrodes are of stainless steel, with the exception of the pole pieces which are cold-rolled steel. The magnetic field is maintained by two solenoids located on either side of the discharge tube. The field is quite uniform inside the discharge volume and can be varied between zero and about 800 gauss. The gun operates on three NJE power supplies, 0 - 20 kv at 0 - 10 ma, 0 - 5 kv at 0 - 100 ma, and 0 - 32 v at 0 - 10 amps. The pressure inside the discharge tube is monitored by a Phillips gauge. Hydrogen gas is admitted to the tube by a Granville-Phillips variable leak.

The extraction hole in the lower cathode is $1/8$ " in diameter and the cathode is supported by glass tubing. Thus the region above this electrode is isolated

from the volume below it, except for the hole. Since the impedance to gas flow of this hole is quite high this arrangement eliminates the need for long tubing to achieve large pressure differences between the gun and the region underneath.

The extracted beam is measured by a Faraday cup 1" in diameter and 2" long located several inches below the lower pole. At the entrance to the cup and co-axial with it is a tube 1/2" in diameter and 1" long which can be made negative with respect to the cup to repel secondary electrons emitted back to the cup. Currents are measured using a Keithley electrometer.

The extracted ion current has been found to be very sensitive to the voltages applied to the various electrodes and to the magnetic field. The ion current and the discharge will change by a large amount or even go out if the fields are not adjusted carefully. However, once the power supplies are warmed up the ion current is quite stable and has been held to within 5% of a given value for 72 hours. The beam current is roughly proportional to the gas pressure in the discharge tube (See Figure 5). A typical operating pressure is about 1×10^{-4} mm Hg.

The ions appear to emerge from the magnetic field in a ~~tight beam about~~ 1/8" in diameter at the lower pole and with an angular width of about $1-1/2^\circ$.

The energy distribution of ions in the beam was measured by monitoring the current to the collector cup while varying the voltage E_s on the suppressor tube between -22.5 v and the anode voltage. Differentiating the curve of the current to the collector cup vs. E_s then gave the distribution of energies in the proton beam (See Figures 6 and 7). The protons appear to be fairly monoenergetic. The energy distribution of ions emerging from the lower cathode is peaked at about 90% of the anode voltage with a spread of about $\pm 10\%$ around this energy.

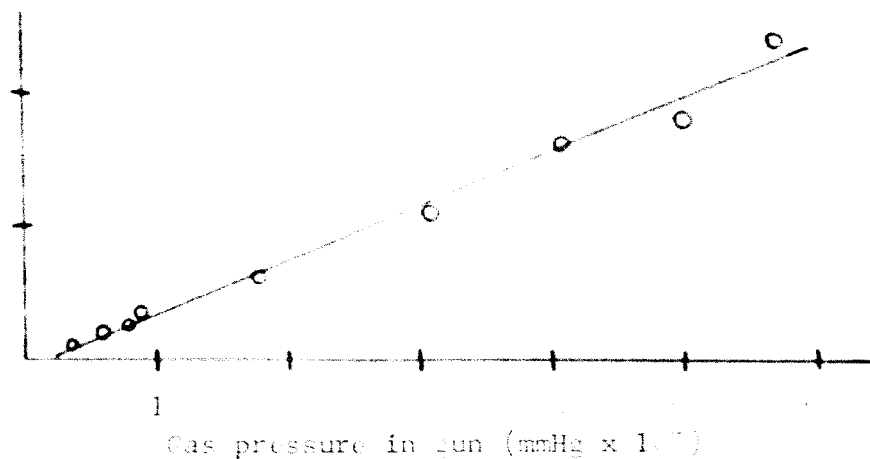


Fig. 5. Extracted proton current vs. gas pressure in discharge tube.

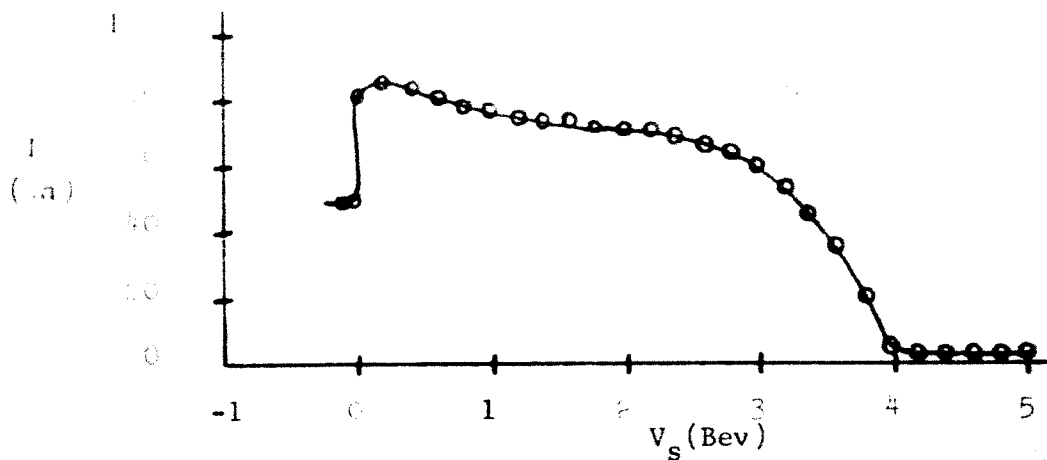


Fig. 6. Current to collector cup vs. voltage on suppressor tube with 3.9 kv on the anode.

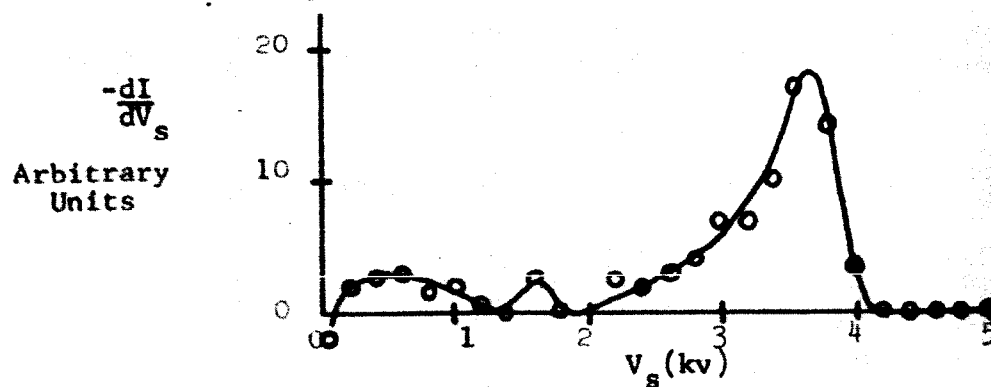


Fig. 7. Distribution of energy in the proton beam (derivative of Figure 6).

The proton gun is designed to be mounted on top of the UHV chamber. An Ultevac ion pump will be used for differential pumping. Part of the tube isolating the UHV from the gun will also be used as an einzel lens to control the width of the proton beam. A small electron gun will be placed inside the UHV; its purpose will be to spray electrons over the surfaces of insulators being bombarded to prevent their charging up to high electrostatic potentials while being irradiated with protons.

In the near future the lateral distribution of protons across the beam will be measured and the contamination of other ions besides H^+ will be estimated.

The proton gun and its associated equipment is shown in Figures 8 and 9.

5. Photometer. The photometric apparatus used for investigating the light-reflecting properties of various surfaces is based on a design by Kalmus (60). The surface being studied is illuminated by a modulated light source and is observed by a phototube and narrow band amplifier peaked at the modulating frequency. Thus this apparatus can be used in a lighted room.

The light source is an S6 type lamp, the filament of which forms the plate load of one side of a multivibrator which is set to run at 20 cps and synched by the 60 cps line frequency. The square wave of current through the lamp causes its light output to vary approximately sinusoidally. The lamp is housed in a box containing condensing and focussing lenses in an arrangement similar to that in a slide projector. This projector throws an evenly illuminated spot of light about $1/2''$ in diameter on a surface 1' away. The spot of light is looked at by a 1P42 type photoelectric tube, the output of which is fed into an AC amplifier. The amplifier contains a bridged-T RC filter network which passes 20 cps and rejects 120 cps to eliminate any unwanted signal from the room lighting. The output appears as a deflection on an ammeter.

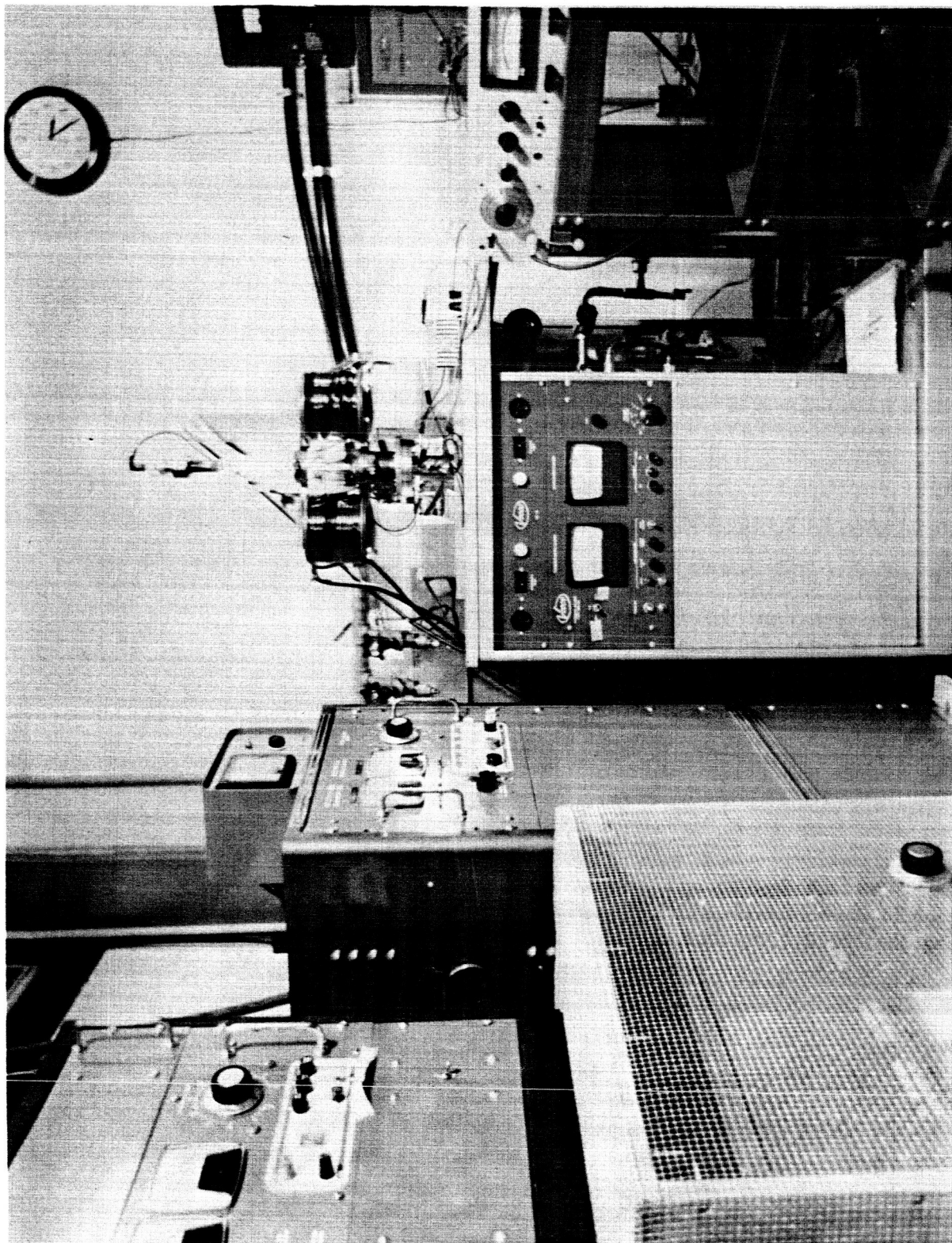


Fig. 8. Proton Gun and Auxiliary Equipment

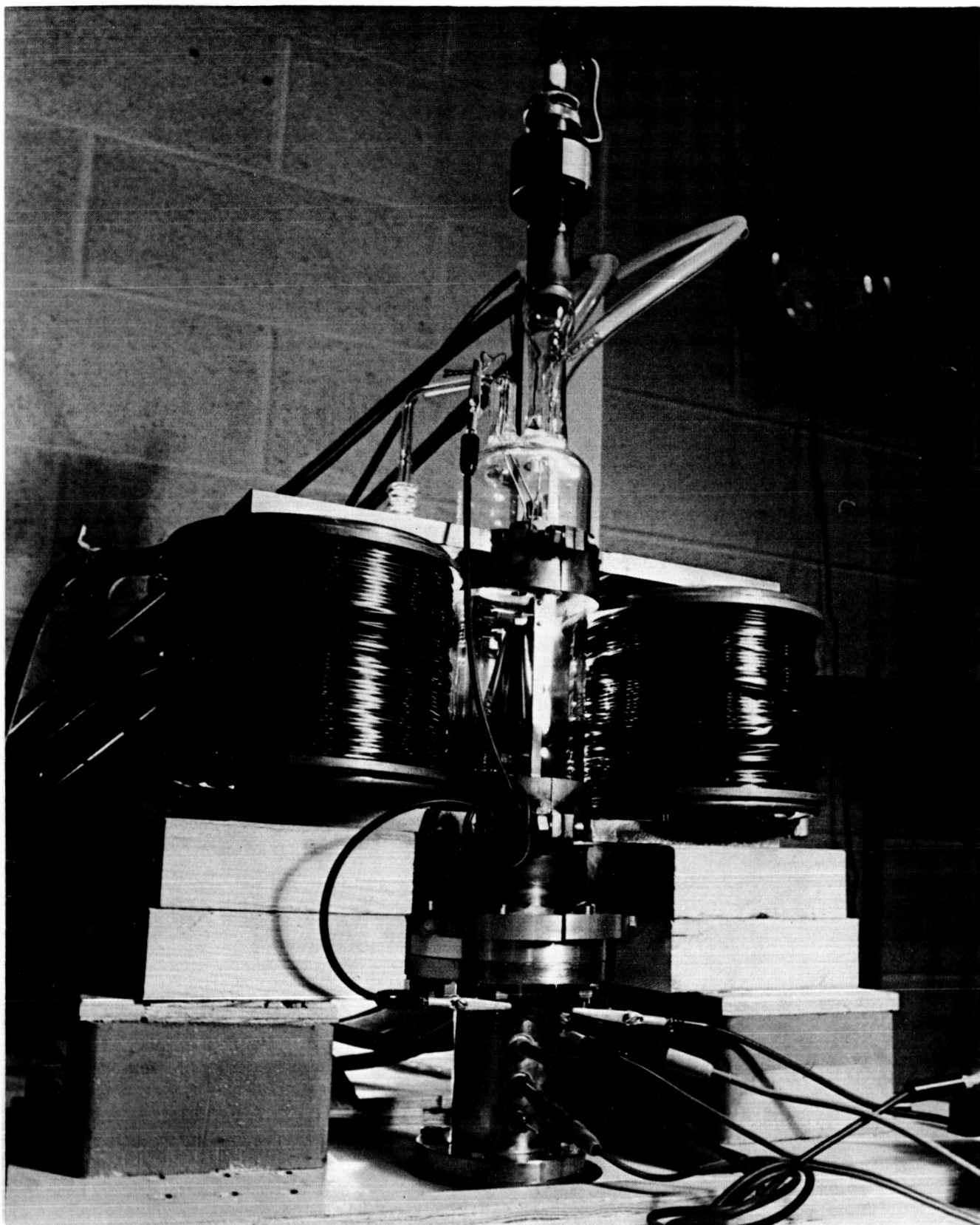


Fig. 9. Proton Gun Assembly

A polaroid can be placed in front of the phototube and rotated to detect any polarization of light produced by the surface. The output meter has a signal-suppress feature which allows most of the incoming signal to be cancelled. The sensitivity of the meter can then be increased to allow small variations in intensity of the signal to be read with precision. Thus a small amount of polarization can be easily measured.

The source and phototube are mounted on arms which can be rotated around a common axis passing through the surface being measured. Thus the angles of incidence and reflection always remain in the same plane in this arrangement. This corresponds to points on the equator on the moon. In the future a minor change will allow the surface to be illuminated and observed obliquely to simulate points off the lunar equator. The apparatus is shown in Figure 10.

6. Miscellaneous. Other important items are described below.

Flour sifter: This is a device for depositing rock dust into various containers in vacuo. It consists of a box containing several trays onto which the rock dust is sprinkled prior to evacuating the UHV. After evacuation and bakeout the dust is allowed to fall into a cup which has a screen for the bottom. The rock powder can be sifted from this cup.

Vacuum pumping station: Also in the laboratory is a Veeco S-9 mobile vacuum pumping station, consisting of a 2" diffusion pump with forepump, cold trap, valves and gauges. It is currently being used to test the proton gun. In the future it will be used in the measurement of secondary emission and sputtering coefficients.

Liquid nitrogen dewar: Since the UHV uses liquid nitrogen in rather large quantities a 200 liter container manufactured by the Ronan and Kunzl Co. of Marshall, Michigan, was purchased.



Fig. 10. Photometric Apparatus

Shear box: A shear box was constructed for measuring the interval friction and cohesion of the dust. This is a split box with a cavity $1/2$ " deep and 1" in diameter; the top half of the box can be moved with respect to the bottom half and the shear resistance of dust deposited in the box measured as a function of normal loading.

The remote hook, part of the flour sifter and the shear box can be seen in place prior to lowering the bell jar in Figure 11.

C. Experiments and Results

The experiments reported here were, with the exception of the photometric measurements, done in the short length of time since arrival of the UHV system and were designed primarily to test the apparatus. All results and conclusions should therefore be regarded as preliminary and will undoubtedly be modified in the future.

1. Erosion. Two specimens of rock were polished and then irradiated by a beam of 9 kv protons, after which they were inspected for evidences of possible erosion. A disk of mica about .010" thick was bombarded at a proton current density of $36 \mu\text{a}/\text{cm}^2$ for 35 hours. This would be equivalent to a period of about 5000 years for a rock located on the lunar equator. A $1/16$ " thick disk of olivine-bearing rock from North Carolina was irradiated at a current density of $120 \mu\text{a}/\text{cm}^2$ for 72 hours, equivalent to 31,000 years on the moon. In both cases the gas pressure at the rock was less than 1×10^{-5} mm Hg. The rock specimens were placed at the bottom of the collector cup used previously to measure the beam current. A heated tungsten filament was also placed in the cup above and to one side of the rock to supply electrons to neutralize any surface charge which might build up in the rock.

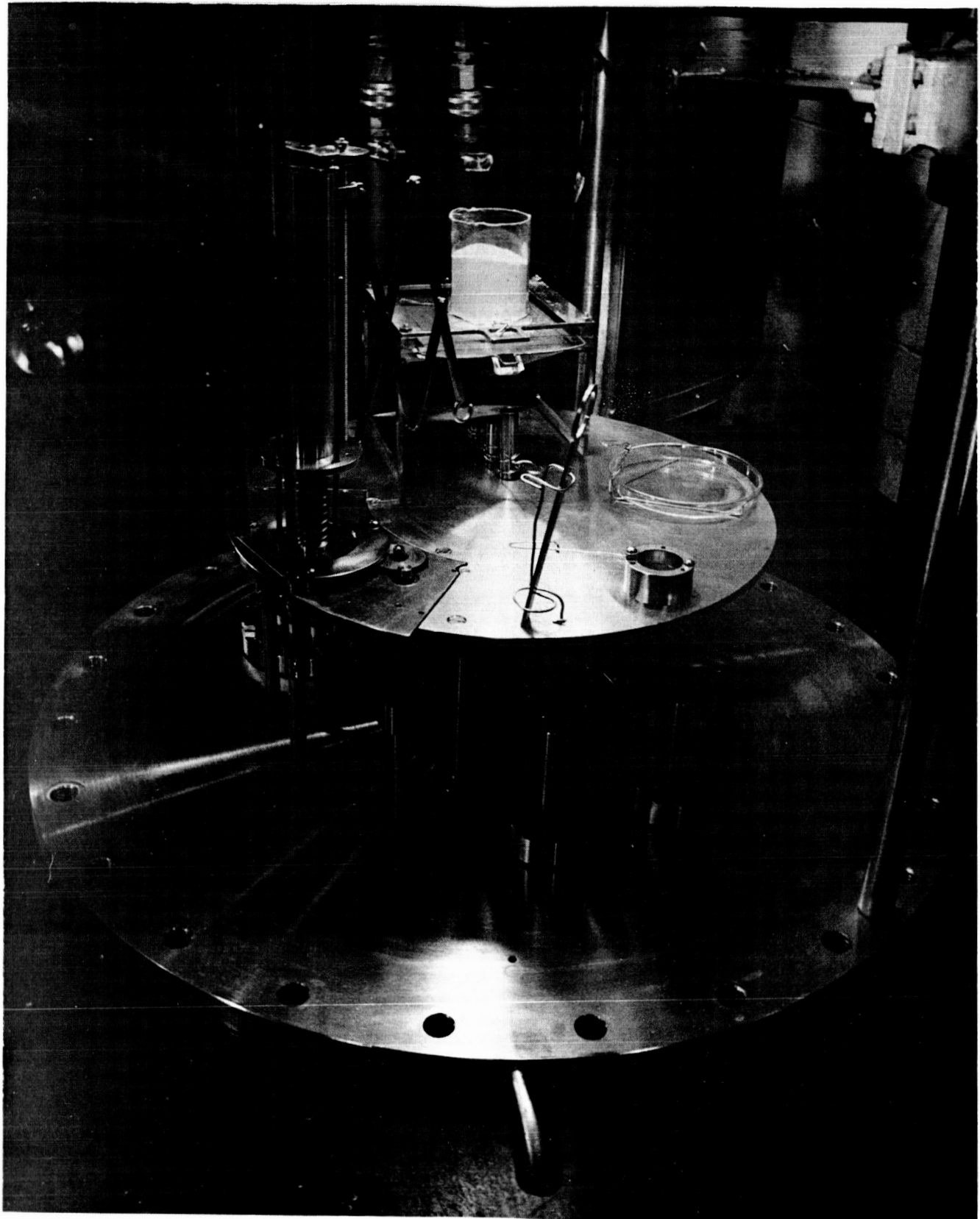


Fig. 11. Remote Arm and Associated Experimental Apparatus

After irradiation the surfaces were removed and examined microscopically. Microphotographs of the two types of rocks are shown in Figures 12-15. No direct evidence for the formation of dust was apparent. Some indirect evidence is presented below.

The mica is a mineral containing Al_2O_3 and SiO_2 . It cleaves easily into smooth polished planes. Before irradiation the specimen was clear and transparent. Under the microscope a few cracks could be seen running across the specimen but otherwise the surface was unmarked. After proton bombardment the upper layer of the irradiated portion was pitted and scarred. It was discolored and was no longer transparent. The surface appeared as if pieces had chipped off, although no traces of such chips could be found. The surface exhibited interference fringes indicating that a thin layer had pulled away from the underlying layers. This could have been due to expansion of the lattice due to the formation of interstitials and dislocations, as discussed previously. It could also have been caused by air trapped between two cleavage planes expanding under the heat of bombardment and forcing the uppermost plane away from the rest of the rock. The irradiated mineral appeared brittle and could easily be chipped and removed from the surface. The damaged layer was about 5μ thick.

The olivine specimen was a polycrystalline rock containing four different minerals. Most of the material was olivine ($(\text{Mg}, \text{Fe}) \text{SiO}_2$) in the form of transparent greenish crystals about 200μ in diameter imbedded in a matrix of greenish serpentine (a hydrated form of olivine). Running through the stone were streaks and blotches of talc (MgO and SiO_2) and there were occasional specks of chromite (FeO and Cr_2O_3). After bombardment the olivine crystals had turned a golden color and had lost some of their transparency. The serpentine appeared to have been eroded away to a considerable depth leaving the olivine standing in relief above the surface. It had also turned a dark grayish in

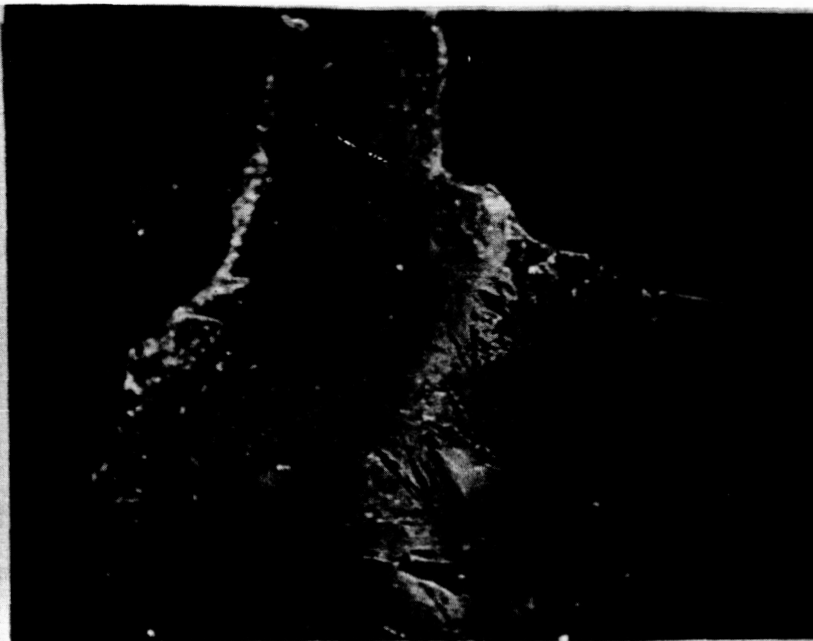


Fig. 12. Mica after proton bombardment. The distance between lines is 140μ .



Fig. 13. Irradiated and unirradiated specimens of olivine-bearing rock. The irradiated rock is at the top. Note the general darkening caused by the proton bombardment.



Fig. 14. Olivine-bearing rock before irradiation.

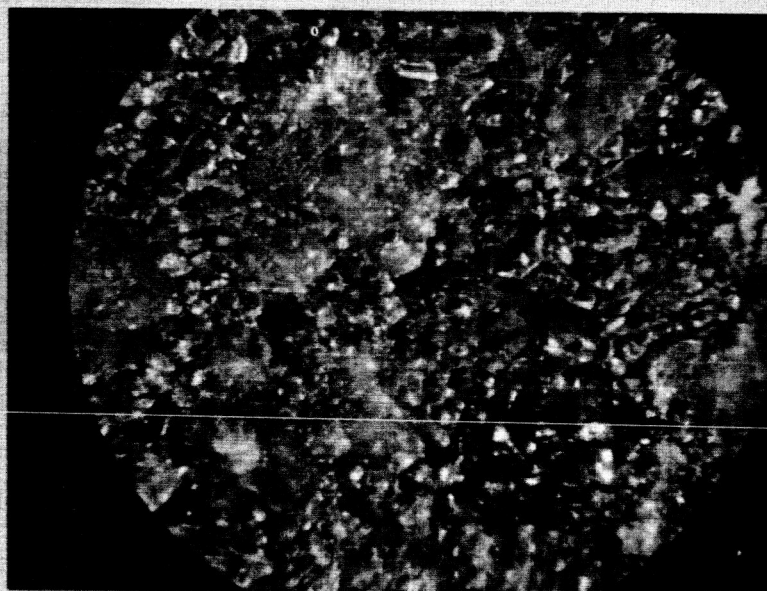


Fig. 15. Olivine-bearing rock after proton bombardment. The large crystals are about 200 μ across.

color. The talc and chromite seemed unaffected by the bombardment. The olivine crystals on the surface were still tightly cemented to the rest of the rock.

The preliminary conclusion which can be drawn from this experiment is that formation of dust by proton bombardment of minerals does not seem significant, although these crude experiments should be repeated more quantitatively before a definite statement can be made. An upper limit to the erosion rate on the moon of about 1μ per 1000 years by this mechanism is indicated from these irradiations. At this rate an amount of material less than one meter thick would have been eroded away from the lunar surface in 10^9 years.

The intense beam did however damage the steel collector cup and the upper surface of the anode. The irradiated portion of the steel was partially covered with a layer of extremely fragile flakes of dust about 5μ thick and 100μ in diameter. These flakes were broken by even the most delicate handling into smaller particles.

2. Properties of vacuum-deposited dust. In the first stages of experimentation to investigate the properties of vacuum-deposited dust an interesting phenomenon appeared. A tube 2" in diameter and whose bottom was covered with a coarse mesh screen was filled to a depth of 2" with dehydrated silica dust consisting of 1 - 10μ size particles. The tube rested on a plate which could be removed. A thick wire could then be drawn across the upper surface of the screen to force powder through the screen. The apparatus was placed inside the UHV chamber and the vacuum pumps were turned on.

As the pressure was slowly reduced the dust could be seen to outgas. Miniature volcanos and geysers of dust were observed. After these disturbances had subsided the pressure was reduced to about one micron and operation of the flour sifter was attempted. When the lower plate was removed and the dust

was disturbed by the wire, the dust seemed almost to explode. Silica powder was expelled violently from the container in every direction, showing that some gas or volatile constituent had remained trapped between the dust grains. Evidently only the upper surface of the powder had outgassed. This phenomenon needs to be investigated further; in particular, the transmission rates of gases through a layer of dust, one surface of which is a vacuum, should be measured, and the possible effects of any trapping of gases under the lunar surface should be estimated.

The density, compressibility, cohesion and internal friction of rock powders deposited in air, in low vacuum, and in high vacuum after prolonged bakeout will be measured and reported in the near future.

3. Transport. Since the tube and flange which will connect the proton gun to the UHV are not yet completed, no dust could be irradiated to study possible transport rates.

The secondary emission measurements have not yet been made. However, some indication as to the value of the secondary electron emission coefficient for protons on metals can be estimated from Figure 6. When V_g was 22.5 v negative with respect to the collector cup no secondary electrons could leave the cup and the current to the cup was 52 μ a. When V_g was about 300 v positive with respect to the cup the current to the cup was a maximum, presumably because all secondary electrons were attracted away from the cup. This current to the cup was due both to the protons and to the secondary electrons. The collector current at this time was 86 μ a. Thus the secondary electron yield for 4 kv protons on steel is of the order of $Y = (86 - 52)/52 = 0.7$ electrons per proton.

4. Photometric studies.

a. Introduction: A series of photometric measurements of the law of light reflection from various surfaces has been initiated for the purpose of matching the law of reflection from the lunar surface. It is expected that a close match to the lunar reflection curve will provide significant information on the nature and micro-structure of the lunar surface layer.

Several previous investigations have been made along these general lines. Of particular interest are the experiments of Bennett (39), of Van Diggelen (40), and of Sharonov, et al (42). Bennett obtained curves of the reflection from some 50 points on the lunar surface and compared his experimental results to a theoretical model of the surface. This model was of a diffusely reflecting plane surface pitted with hemi-ellipsoidal cups which reflect light uniformly into all angles, the amount of light varying directly as the visible portion of the illuminated inner surface of the cups. The agreement of this model with the lunar data is - as Bennett points out - rather poor.

Van Diggelen summarized the work of previous investigators and compared their data with his own. He found quite good agreement between the data of different workers. He also obtained the reflection law from several different surfaces: volcanic ash, a surface of glass beads, a flat metal plate covered with magnesium oxide smoke, a whitened metal plate partly covered with pits of a form proposed by Tschunko, a surface with humps, a metal plate on which caraway seeds were glued, the whole being covered with magnesium oxide smoke (to simulate a stony surface), a surface with hemi-ellipsoidal holes, and the surface of the spongy lichen Cladonia Rangiferina. Van Diggelen found the best agreement with the lunar data for the surface of the lichen.

Sharonov, et al (42) claims to have investigated "thousands" of different surfaces in an attempt to match the lunar data, but that none of the surfaces he examined provided a particularly good site to the data. Apparently much of this work is unpublished so that it is impossible, at present, to estimate the value of this work.

b. Experimental procedure and data reduction: The experimental data given in this section was taken by Hugh Van Horn and portions of this section were written by him. The 20 cps photometer described elsewhere in this report was used to obtain the reflection law from various surfaces. This preliminary study was aimed at discovering the effects of the structure of the surface on the form of the reflection law; consequently little attention was paid to other factors such as color, chemical composition, etc.

The reflection law from the surface was measured with the photometer in two positions. For vertical observation of the surface, the position of the light source was varied from 5° with the vertical to 70° with the vertical in 10° intervals. For 60° observation of the surface (the photometer set at 60° from the vertical), the intensity of reflected light was measured with the light source varying from -70° (light source on the opposite side of the vertical from the photometer) to $+70^{\circ}$ (light source on the same side of the vertical as the photometer).

A noise figure was obtained after each run by blocking off the light source and reading the meter of the photometer. A standard surface was prepared by smoking a $1/4$ " thick glass plate with the white smoke of burning magnesium. In order to eliminate any effects of non-uniform illumination it was assumed that this surface was a Lambert surface (i.e., a perfectly diffusely-reflecting surface (40)), and all readings of the photometer were corrected to this standard. All surfaces were measured at least twice.

It is desirable to report the data as "reflected intensity per unit cross-section of reflected beam," as this provides immediate comparison with the lunar data; hence the photometric measurements were multiplied by the cosine of the angle of incidence of the light. This correction made the graphs of the reflection laws of the various samples directly comparable with the law of reflection from the moon.

c. Theoretical considerations: It has been suggested that the surface layer of the moon may have one of the following forms: (i) dust, (ii) foam, (iii) volcanic glass, or (iv) whiskers. In order to check the effects of these structural forms on the reflection law, surfaces were selected primarily on the basis of surface structure, and only secondarily on the basis of composition. We have extended the work of Bennett and Van Diggelen on the reflections from artificial surfaces by constructing such surfaces as a wire screen suspended above a metal plate, the whole being smoked with magnesium oxide, a surface consisting of straight pins standing vertically and enmeshed in a mat of glass wool, the resulting structure being coated with magnesium oxide smoke, and a plane surface cut from a block of styrofoam.

The surfaces for which reflection laws were obtained may be grouped in the following categories:

Category I: "Artificial surfaces" designed to test the effect of overhangs, vertical walls, etc. on the reflection law.

Category II: Needle-like or whisker-like surfaces of various degrees of packing and particle size.

Category III: Compacted surfaces of SiO_2 powders of varying particle size to test the effect of particle size on the reflection laws.

Category IV: Fibrous surfaces of various fineness and composition.

Category V: Miscellaneous rock powders and chemical compounds.

d. Photometric observations: The reflection curves of various selected surfaces together with photographs of these surfaces are given in Figures 16-21. The graph on the left-hand side of each figure is for vertical observation of the surface, while the graph on the right-hand side is for observation of the surface at 60° from the vertical. In the latter graph, the angles of illumination recorded as negative are those for which the light source is on the opposite side of the normal to the surface from the observer.

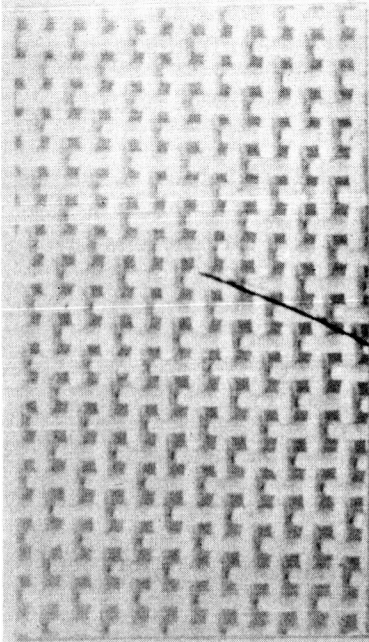
On the same scales, the Lambert reflection law (dotted lines) and the reflection law for a comparable point on the lunar surface as given by Van Diggelen (40) (dashed lines) are plotted. The circles and solid curves are the experimental data.

The strong "bright shadow" effect observed on the moon is clearly evident in the curves for both angles of observation. This effect arises in the following manner:

In an intricately structured surface with many overhangs, illumination of the surface from any angle will cast shadows of the overhanging parts onto the underlying areas. Only when the angles of illumination and observation are the same (so that the observer is looking parallel to the incident beam of light) will the shadows be unseen; any angular separation of the light source and observer will allow some portion of unilluminated surface to be seen. Consequently, the surface will appear brightest when the line of sight is parallel to the incident beam, independently of the angle between the light source or observer and the surface. The surface will appear darker for any other angular relation between the source and observer with the amount of darkening increasing with increasing angular separation.

It is important to note that the strong "bright shadow" effect as described above can only be demonstrated by surfaces with overhang; non-

REFLECTION LAW OF
A MgO-COATED SCREEN
SUSPENDED ABOVE A
MgO-COATED PLATE AT
A DISTANCE EQUAL TO
THE WIRE DIAMETER



MICRORELIEF OF COATED SCREEN COMPARED
WITH 0.005" DIA. WIRE

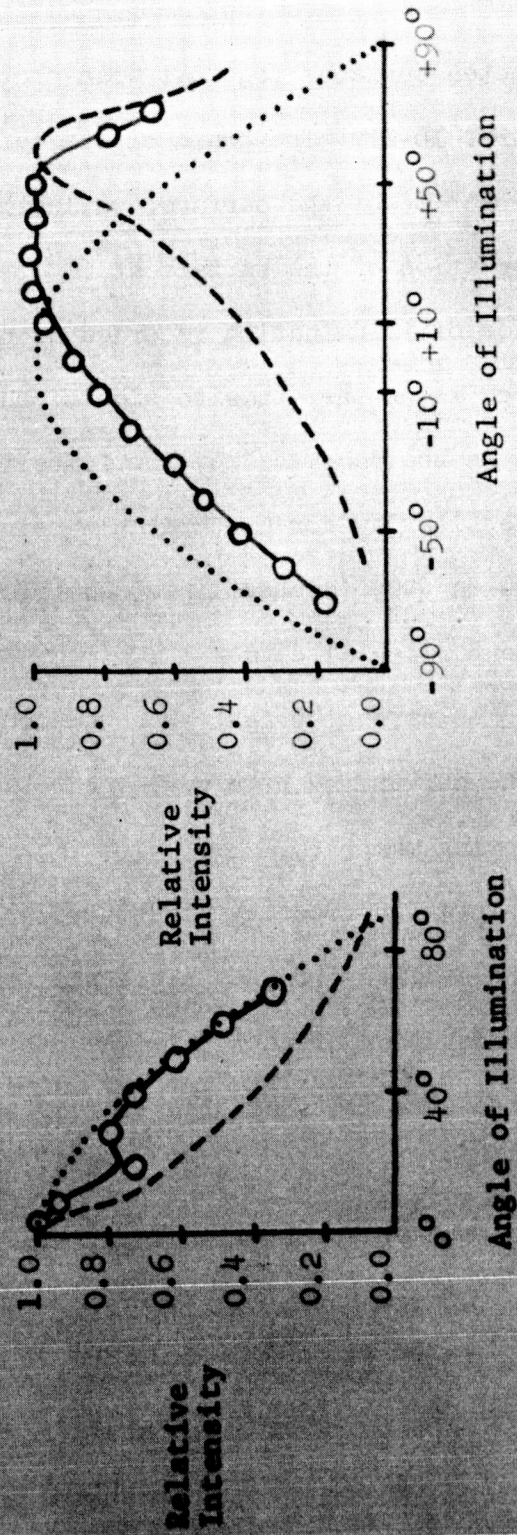
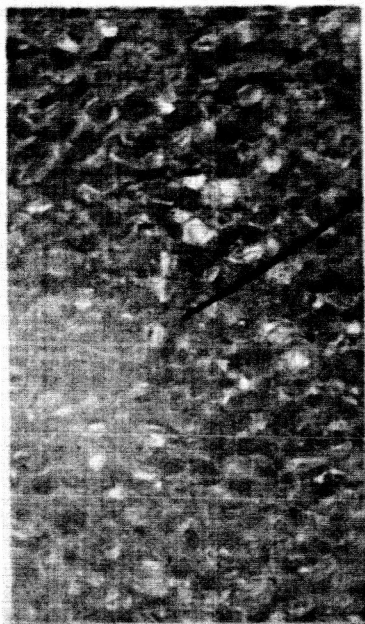


FIGURE 16

REFLECTION LAW OF
THE SURFACE OF A
STYROFOAM BLOCK



MICRORELIEF OF STYROFOAM COMPARED
WITH 0.005" DIA. WIRE

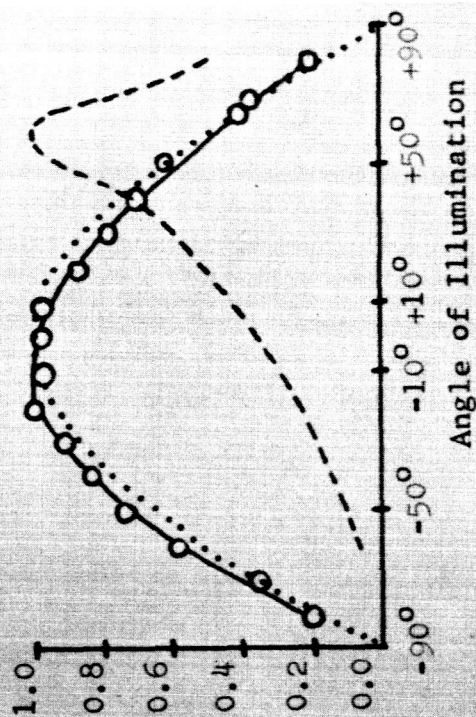
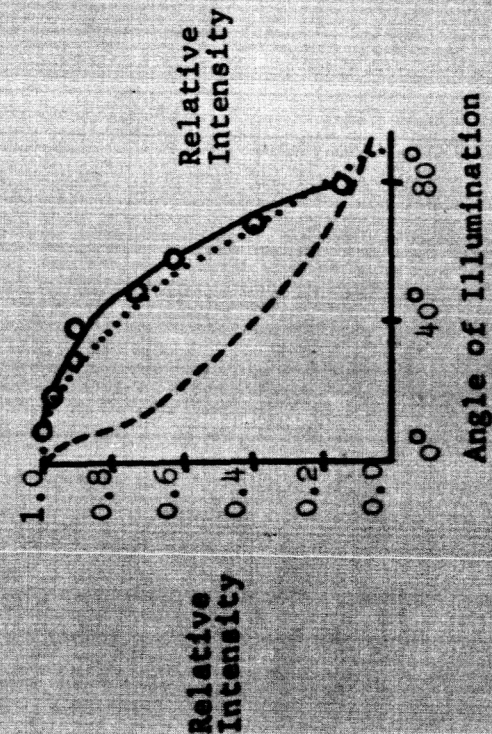
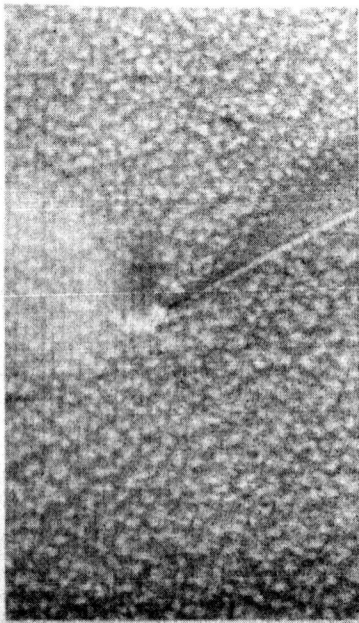


FIGURE 17

REFLECTION LAW OF
A SURFACE OF ICE
WHISKERS SUBLIMED
ON A COPPER PLATE



MICRORELIEF OF ICE WHISKERS COMPARED
WITH 0.005" DIA. WIRE

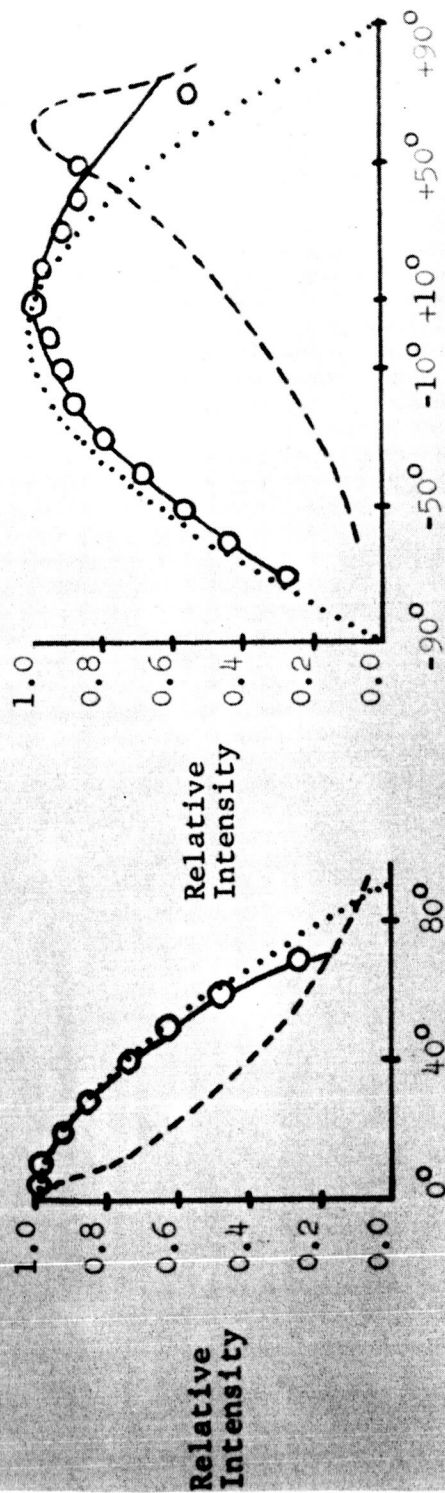


FIGURE 18

REFLECTION LAW OF
A SURFACE OF
LAWN GRASS, TWO TO
THREE INCHES LONG



MICRORELIEF OF GRASS COMPARED WITH
0.005" DIA. WIRE

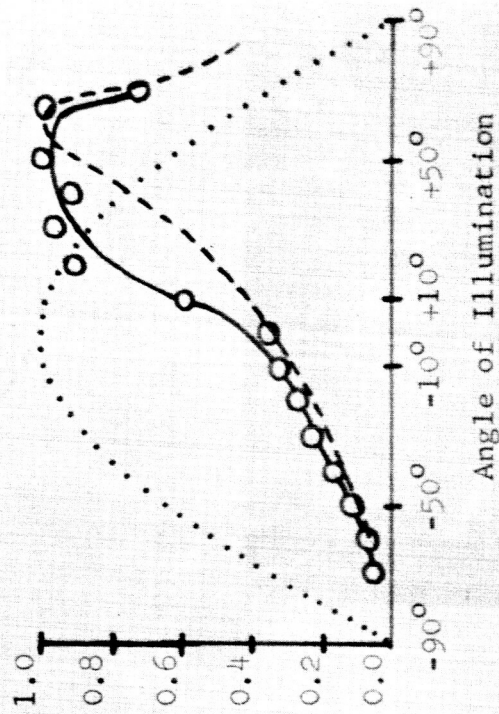
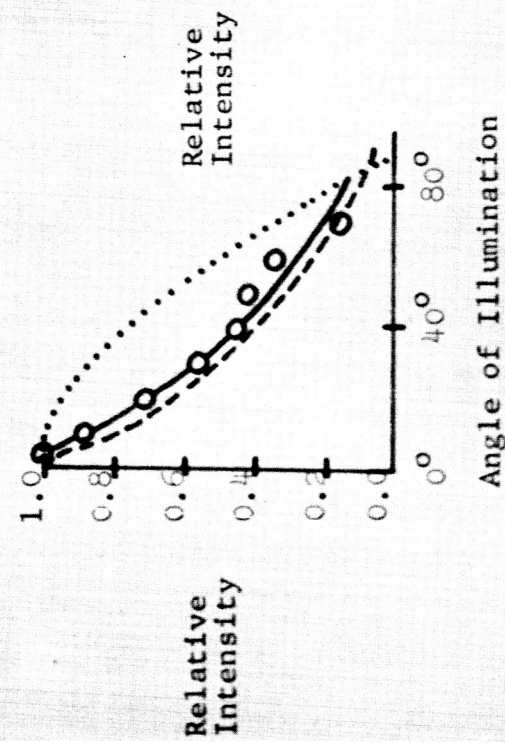


FIGURE 19

REFLECTION LAW OF
A SURFACE OF
LAWN GRASS CLIPPED
TO ONE INCH LENGTH



MICRORELIEF OF CLIPPED GRASS COMPARED
WITH 0.005" DIA. WIRE

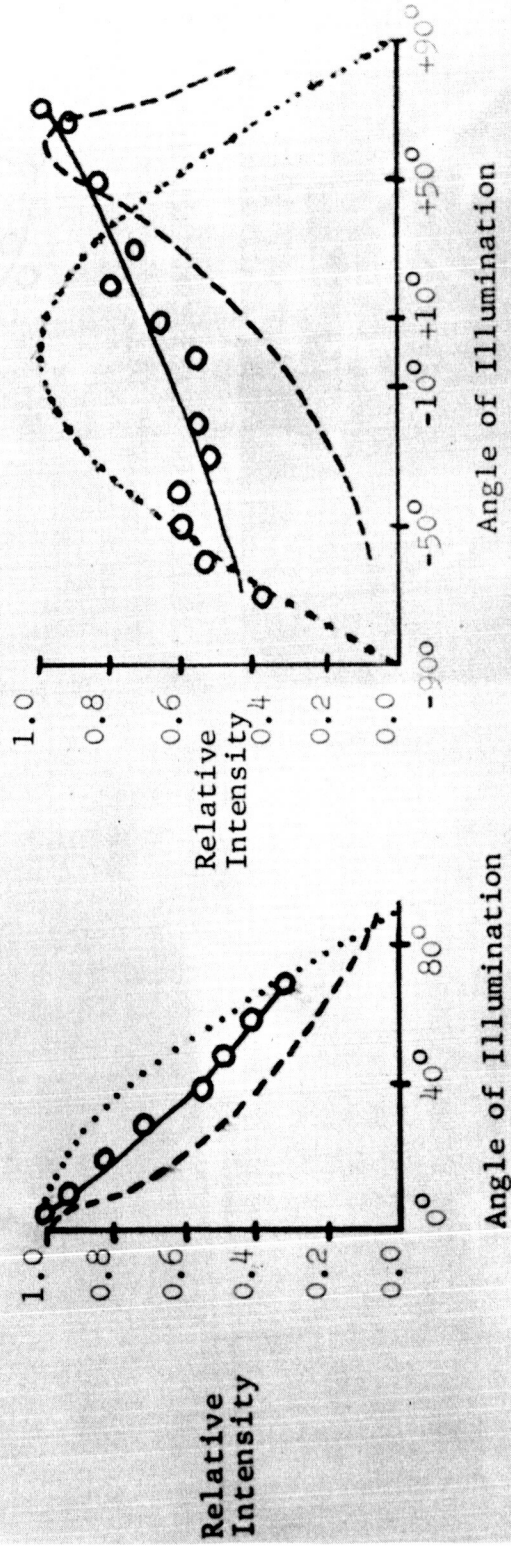
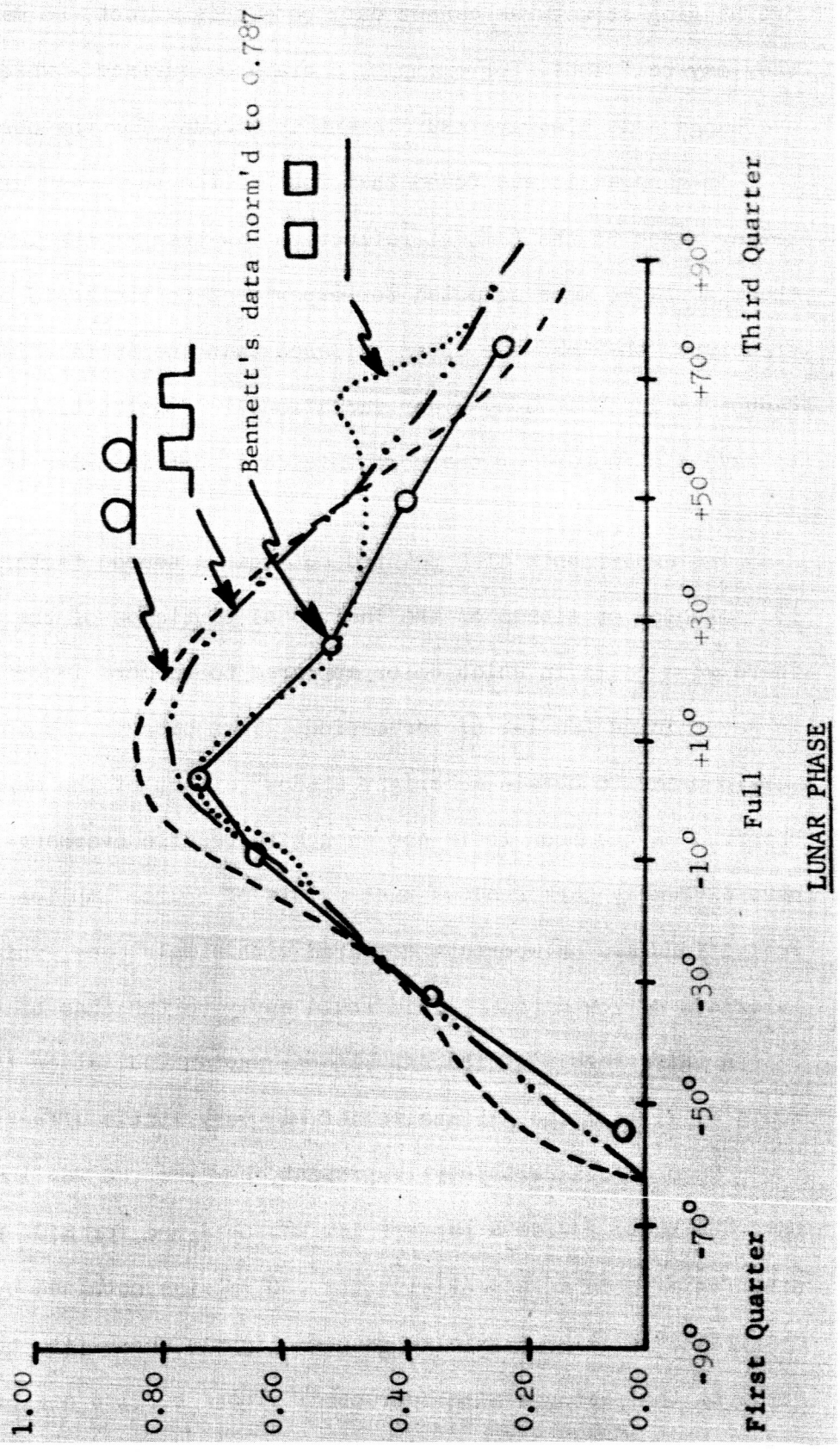


FIGURE 20

THEORETICAL REFLECTION LAWS FOR VARIOUS
 DIFFUSELY REFLECTING STRUCTURED SURFACES
 COMPARED WITH BENNETT'S DATA FOR REFLECTIONS
 FROM A RAY OF COPERNICUS

FIGURE 21



overhanging structures cannot duplicate this effect, no matter how rough they may be. Thus, for example, a cratered surface - which of course has no overhangs - is clearly insufficient to account for the observed strong effect.

In general it was found that most of the surfaces used provided a much better match to the Lambert reflection law than to the lunar data. Since these surfaces were selected for experiment on the basis of differing surface structure, they provide clear evidence that the surface layer of the moon cannot be duplicated by minor variations in construction. Indeed it is necessary to have a structure of the most intricate sort in order to match the lunar curves.

The experiments also pointed out that a second factor of great importance is the color or albedo of the individual particles of the surface. In fact there were cases in which color appeared to be more important than structure in determining the law of reflection. This behavior is to be expected, however, for in order to obtain a "bright shadow" effect of the magnitude of that observed on the moon it is not enough to require overhangs. One must also have extremely dark shadows cast. This of course implies that multiple reflections are unimportant compared with single ones, which will be true for materials of low albedo. This would apply to the case of the moon.

A third result of the experiments was an indication that the absolute scale of size of the surface relief has very little effect on the reflection law. Some effect certainly is present, however, as was indicated by the fact that the best fit to a Lambert law was obtained for SiO_2 particles of .05 mm size (this is in agreement with the .06 mm size obtained by Barbashev and Chakirda). Smaller particles gave a slightly worse fit, the agreement becoming worse as the particle size decreased. These results are probably caused by diffraction effects, which appear not to occur to any significant degree on the moon.

e. Conclusions: On the basis of these experiments, we are led to suppose that the lunar surface must have an extremely intricate structure which makes for a substantial amount of shadowing. The material of which this bizarre structure is composed must be intrinsically quite dark and the scale of the irregularities must be large enough so that diffraction effects do not destroy shadows. The characteristic scale for these surface features must thus lie between several microns and several centimeters, to occur both with the optical and the radar evidence. The only surfaces which are likely to be able to assume such forms are whiskery, crystalline surfaces, dark foams, and dust deposited in vacuum under low gravity. In any event, it is certain that no amount of cratering of the surface on any scale whatever can possibly duplicate the strong observed "bright shadow" effect.

The work under way now is intended to find out whether vacuum deposited dust can make a surface of porous, fragile structures as seems to be required. Also the properties of dark foams and slags will be investigated.

The photometer will also be used to study the reflection polarization effects, and to find the materials that match the lunar surface in this respect. A surface structure of roughness on a scale comparable with the wavelength of light is required for this. The combination of these properties will narrow down still further the range of surface types that may be thought of as composing the lunar surface.

BIBLIOGRAPHY

1. Urey, The Planets, Yale, 1961, Chapter 2.
2. Elsmore, Paris Symposium on Radio Astronomy (Bracewell, ed.), paper 6, Stanford University Press, 47 (1959).
3. Blackwell and Ingham, MNRAS, 122, 113-176 (1961).
4. Baldwin, The Face of the Moon, University of Chicago Press, (1958).
5. Senior and Siegel, J. Research NBS, 64D, 217 (1960).
6. Straighton and Olbert, U. of Texas Elec. Eng. Res. Lab. Report, 5-38 (1959).
7. Hughes, Nature, 186, 873 (1960).
8. Yaplee, et al, Proc. IRE, 46, 293 (1958).
9. Pettengill, Proc. IRE, 48, 933 (1960).
10. Leadabrand, et al, J. Geophys. Res., 65, 3071 (1960).
11. Evans, Proc. Phys. Soc., B70, 1105 (1957).
12. Hargreaves, Proc. Phys. Soc., 73, 536 (1959).
13. Brown and Evans, Radio Astronomy, Cambridge, 1957, page 409.
14. Brunschwig, et al, U. of Mich. Elec. Eng. Dept. Report 3544-F (1960).
15. Handbook of Chemistry and Physics, Chemical Rubber Publ. Co. (1960).
16. Petit and Nicholson, Ap. J., 71, 102 (1930).
17. Shorthill, et al, PASP, 72, 481 (1960).
18. Sinton, Bull. Lowell Obs., No. 108, 5, 25 (1960).
19. Geoffrion, et al, Bull. Lowell Obs., No. 106, 5, 1 (1960).
20. Sinton, J. Opt. Soc. Amer., 45, 975 (1955).
21. Coates, Ap. J., 133, 723 (1961).
22. Tyler, et al, Bull. Am. Phys. Soc., 3, 301 (1958).
23. Gibson, Proc. IRE, 46, 280 (1958).
24. Salomonovitch, Astron. Zh., 35, 129 (1958).
25. Amenitskii, et al, Sov. Astr. AJ, 4, 177 (1960).
26. Piddington and Minnet, Austral. J. Sci. Res., A2, 63 (1949).

27. Zelinskii, et al, Sov. Astr. AJ, 3, 628 (1960).
28. Grebenkemper, Naval Res. Lab. Report 5151 (1960).
29. Troitsky and Khaikin, Radio Astronomy, Cambridge, 1957, p. 406.
30. Castelli, et al, A. J., 65, 485 (1960).
31. Mezger and Strassl, Plan. and Space Sci., 1, 213 (1959).
32. Seeger, et al, Ap. J., 126, 585 (1957).
33. Jaeger and Harper, Nature, 166, 1026 (1950).
34. Wesselink, B.A.N., 10, 351 (1948).
35. Giraud, U. of Mich. Elec. Eng. Dept. Report 03544-1-T (1960).
36. Stair and Johnston, J. Res. NBS, 51, 81 (1953).
37. Wood, Researches in Physical Optics, Columbia, New York, 1913, Vol. I.
38. Kuiper, J. Geophys. Res., 64, 1713 (1959).
39. Bennet, Ap. J., 88, 1 (1938).
40. Van Diggelen, Photometric Properties of Lunar Crater Floors, Univ. Groningen (1959).
41. Sytinskaya, Sov. Astr. AJ, 3, 310 (1959).
42. Barabashov and Chekirda, Sov. Astr. AJ, 3, 827 (1960).
43. Lyot, Compte Rendus, 178, 1796 (1924).
44. Dollfus, Supplements aux Annales d'Astrophysique Fascicule, No. 4 (1957).
45. Dollfus, Annales d'Astrophysique, 83 (1956).
46. Wright, Proc. Nat. Acad. Sci., 13, 535 (1927).
47. Dietz, Scientific American, Aug., 1961, p. 50.
48. Symposium on Tecktites, Geochim. et Cosmochim. Acta, 14 (1958).
49. Firsoff, The Strange World of the Moon, London, Hutchinson (1959).
50. Charters, Scientific American, October, 1960, p. 128.
51. Private communication from Martin Harwit.
52. Moore, Amer. Scientist, 48, 109 (1960).
53. Dubin, Space Research, Bijl, Ed., North-Holland, 1960, p. 1042.

54. International Critical Tables, II, 315 (1929).
55. Handbook of Chemistry and Physics, 41st Ed., p. 2284.
56. Gold, MNRAS, 115, 585 (1955).
57. Grannis, Senior Project Report, Cornell University, Dept. of Engineering Physics, 1961.
58. Platt, Science, 127, 1502 (1958).
59. Coates, Ap. J., 133, 723 (1961).
60. Hollister, Ph.D. Thesis, Cornell University, Dept. of Engineering Physics, 1961.
61. Kalmers and Sanders, Electronics, July, 1950, p. 84.